3942 *Macromolecules* **2009**, *42*, 3942–3950
DOI: 10.1021/ma9003715

Macromolecules
ARTICLE

Comb Copolymers with Polystyrene and Polyisoprene Branches: Effect of Block Topology on Film Morphology

David Lanson,[†] Fumi Ariura,[†] Michel Schappacher,[†] Redouane Borsali,*[,‡] and Alain Deffieux*[,†]

[†]*Laboratoire de Chimie des Polymères Organiques, CNRS, Université Bordeaux, ENSCPB, 16 Avenue Pey Berland 33607 PESSAC Cedex, France, and* [‡]*CERMAV, CNRS UPR 5301 and Joseph Fourier University, BP 53, 38041 Grenoble Cedex 9, France*

Received February 18, 2009; Revised Manuscript Received April 29, 2009

ABSTRACT: Comblike copolymers with randomly distributed polystyrene (PS) and polyisoprene (PI) branches, i.e., PCEVE-*g*-(PS,PI), were synthesized by the "grafting onto" technique. The comblike copolymers exhibit a low dispersity, high molar masses, and controlled number of branches. Their characteristics and behavior as isolated objects were investigated as solid molecular deposits, using atomic force microscopy (AFM), and in solution, in a good solvent of the polystyrene and polyisoprene branches, using dynamic light scattering (DLS). AFM experiments show isolated uniform molecules that adopt an ovoïdal conformation whose dimensions are found in good agreement with DLS data. The self-organization of the PS, PI comb copolymers was further studied in the solid state as thin films, using SAXS. The results show that PCEVE-*g*-*(PS,PI) combs yield lamellar biphasic morphologies that were compared to those observed for PCEVE*-g-*(PS*-b-*PI) combs with PS*-b-*PI diblock branches and those known for linear PS*-b-*PI of similar weight compositions*.

Introduction

Over the past years, linear diblock copolymers have attracted considerable attention as building bricks for the development of novel self-assembled materials,[1,2] since it was shown that copolymers with noncompatible blocks can be organized into a large variety of ordered superstructures. The progress made in the past decades in controlling polymerization processes has led to the development of new types of copolymers with branched and hyperbranched architectures[3−6] that can self-organize both intra- and intermolecularly. In this domain, comb copolymers have emerged as one of the simplest models of these branched architectures, which could respond to the needs of polymer materials with new or improved properties. The number of reports on the synthesis of comblike polymers and copolymers has rapidly grown in recent years.[3,6−22] It was already shown that comblike copolymers can self-assemble in solution, forming supramolecular structures.[5,23−34] However, up to now, only few studies have been focused on the investigation of their self-organization properties in the bulk;[35−42] a major part of the reported works concerns simulation studies.

In the present work we have prepared random comblike copolymers constituted of a poly(chloroethyl vinyl ether) backbone bearing randomly distributed polystyrene and polyisoprene branches, i.e., PCEVE-*g*-(PS,PI), as schematically illustrated in Figure 1a. The latter were first characterized as single objects using light scattering techniques and AFM imaging. Their self-organization, in the solid state, as thin film was then investigated using small-angle X-ray (SAXS) and compared to organized nano-organized films of comblike copolymers with PS-*b*-PI diblock branches (Figure 1b), previously synthtesized,[31] and with those of linear PS-*b*-PI diblock copolymers of same PS and PI block molecular weight and composition.

Experimental Section

Materials. Cyclohexane and toluene (99.5%, J.T. Baker, Deventer, The Netherlands) were purified by distillation from calcium hydride and stored from polystyryllithium seeds. Styrene (99%, Sigma-Aldrich Chimie, Saint Quentin Fallavier, France) was purified by distillation from calcium hydride at reduced pressure. *sec*-Butyllithium (1.3 M in cyclohexane, Sigma-Aldrich Chimie, Saint Quentin Fallavier, France) was used as received. All the reactants were stored under dry nitrogen in glass apparatus fitted with PTFE stopcocks.

Polymerization Procedures. *Synthesis of the PCEVE Backbone and the PCEVE-g-PS* Comblike Polymers*. The preparation of these polymers has been described in detail in previous contributions.[8,24,43] Briefly, a poly(chloroethyl vinyl ether), PCEVE, with degree of polymerization $\overline{DP}_{n(PCEVE)} = 230$ and dispersity $\overline{M}_w/\overline{M}_n = 1.03$ was first synthesized by living cationic polymerization of chloroethyl vinyl ether using propyldiethylacetal/trimethylsilyl iodide as initiating system and zinc chloride as catalyst and used as reactive backbone. Living polystyryllithium chains of controlled $\overline{DP}_n$ and narrow dispersity were then prepared in cyclohexane using *sec*-butyllithium (Scheme 1a) and added onto the PCEVE backbone by incremental addition of the living PSLi solution onto a known quantity of PCEVE in cyclohexane solution to form a PS comblike polymer by partial substitution of the chlorides of the PCEVE backbone, PCEVE-*g*-PS* (Scheme 1b). Analysis of PCEVE-*g*-PS* samples taken at different reaction times by size exclusion chromatography (SEC) using both refractive index (RI) and light scattering (LS) detections allowed us to control the PS grafting rate. Selective precipitation of the comb polymer in cyclohexane/heptane allowed recovering the PS comb free of ungrafted and deactivated linear PS (about 10% of the total amount). The yield in recovered PCEVE-*g*-PS* was about 90%. Molar mass and other characteristics are collected in Table 1.

Synthesis of PCEVE-g-(PS,PI) Comblike Copolymers with Randomly Distributed PS and PI Branches. A typical reaction procedure is described below. PCEVE-*g*-PS* comblike polymers (**1**) with $\overline{DP}_{n(PCEVE)} = 230$ and $\overline{DP}_{n(PS)} = 86$ (1.6 g, 1.86×10^{-4} mol in PS branch equiv) is placed in a 500 mL glass reactor fitted with PTFE stopcocks and dissolved in 20 mL of dry toluene. To remove any traces of moisture from the polymer, the

 Published on Web 05/19/2009

solvent is evaporated under vacuum and replaced by a new volume of dry toluene. This operation is repeated twice, and the polymer is finally dissolved into anhydrous toluene (200 mL).

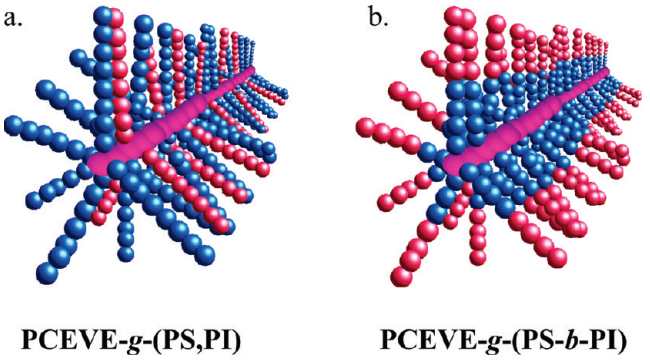

Figure 1. Idealized structure of (a) comblike copolymers with randomly distributed branches and (b) comblike copolymers with diblock branches.

A red solution of polyisoprenyllithium end-capped with one unit of DPE (Scheme 1c), PIDLi, with $\overline{DP}_{n(PI)} = 98$ (microstructure 85% 1,4), previously prepared in toluene using *sec*-butyllithium as initiator, was then incrementally added to the PCEVE-*g*-PS* (Scheme 1d). The rate of PIDLi addition was determined by the disappearance of the coloration of the solution, and PIDLi was added until a fading pink color of the reacting media remained over about a 24 h period. The excess of PIDLi added is easily removed from the comb copolymer by selective precipitation of the polymer solution into a dichloromethane/methanol (1:4) mixture. The yield in recovered PCEVE-*g*-(PS,PI), free of residual ungrafted PS and PI, was about 80%. They were characterized by SEC using RI and laser light scattering detections to determine their apparent and absolute molar masses and by proton ^{1}H NMR to determine their PS and PI composition. Their molar masses and other characteristics are collected in Table 1.

Synthesis of the PCEVE-g-(PS-b-PI) Comblike Block Copolymers. The synthesis of these samples was reported in a previous study.[31] Their characteristics are collected in Table 3. They were used for morphology studies.

Scheme 1. Strategy for the Synthesis of Poly(chloroethyl vinyl ether-*g*-(polystyrene, polyisoprene), Poly(CEVE)-*g*-(PS,PI), Combs (TMEDA = Tetramethylenediamine)

(a) Synthesis of polystyryl-lithium

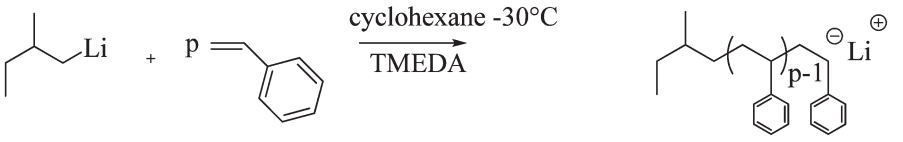

(b) Synthesis of poly(CEVE)-*g*-PS*comb

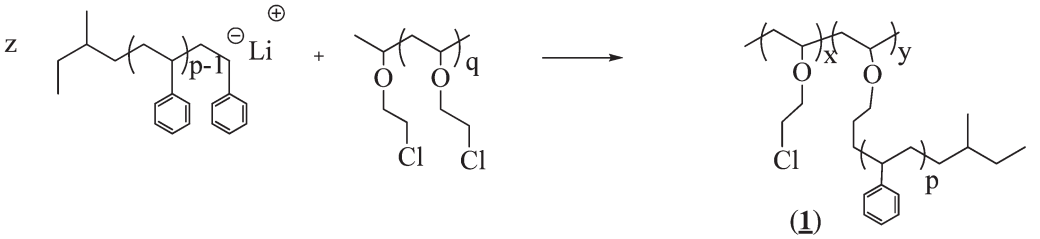

(c) Synthesis of DPE end-capped polyisoprenyl-lithium

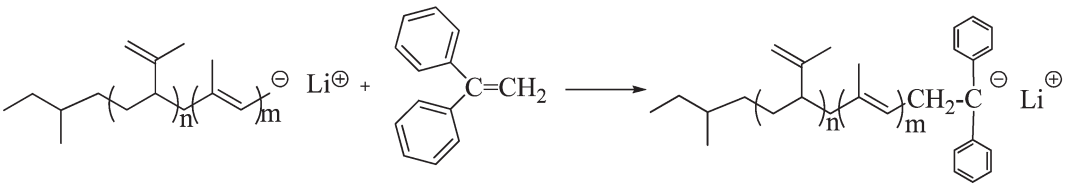

(d) Synthesis of poly(CEVE)-*g*-(PS,PI) comb copolymer

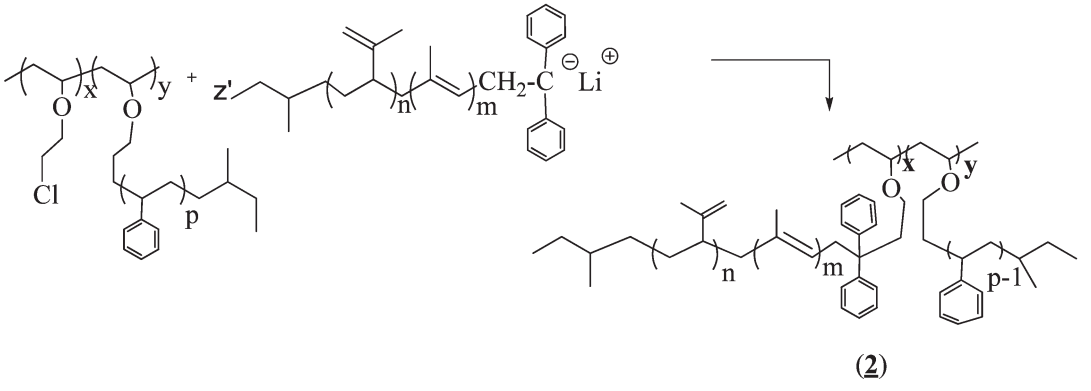

Table 1. Characteristics of Comb Poly(chloroethyl vinyl ether)-*g*-polystyrene* (1) and Comb Copolymers Poly(chloroethyl vinyl ether)-*g*-(polystyrene, polyisoprene) (2a and 2b)

ref no.	constitutive blocks $\overline{DP}_n$ PCEVE−(PS, PI)	$\overline{M}_{w,th}$[a] (g/mol) × 10^{-6}	$\overline{M}_{w,exp}$ (LS)[b] (g/mol) × 10^{-6}	$\overline{M}_w/\overline{M}_n$	grafting yield,[c] % PS	PI	$\Phi_{vPS/PI}$[d]
1	230−(86, 0)	(0.77)	0.93	1.06	45	−	100/0
2a	230−(86, 57)	1.44	1.51	1.08	45	55	60/40
2b	230−(86, 98)	1.79	1.88	1.09	45	55	48/52

[a] Calculated assuming (**1**) $\overline{M}_{w,th} = \overline{M}_{w,PCEVE} + (230 \times \overline{M}_{w,PSX}x\%) - (230 \times 35.5x\%)$ whith x the PS grafting yield and for (**2a** or **2b**) $\overline{M}_{w,th} = \overline{M}_{w,PCEVE} + (230 \times \overline{M}_{w,PSX}x\%$ grafting yield) + $(230 \times \overline{M}_{w,PI}x\%$ grafting yield) − (230 × 35.5). [b] $\overline{M}_{w,exp}$ determined by light scattering (LS) in tetrahydrofuran (THF) at 25 °C: dn/dc = 0.181 for PCEVE-*g*-PS* and dn/dc = 0.165 and 0.135 for PCEVE-*g*-(PS,PI) (**2a**) and (**2b**), respectively. [c] Grafting yield based on the ratio between molar mass determined by SLS and theoretical molar mass $\overline{M}_{w,th}$. [d] $\Phi_{vPS/PI}$ volume fraction of PS and PI determined by ^{1}H NMR. The volume fraction of PCEVE is < 1% and was neglected.

Synthesis of the PS-b-PI Linear Diblock Copolymers. Two samples, PS_{115}-*b*-PI_{175} (**L1**) and PS_{115}-*b*-PI_{65} (**L2**), with low dispersity (< 1.10) were prepared by sequential anionic polymerization of styrene and isoprene initiated by *sec*-butyllithium in cyclohexane in a flamed glass reactor. PS-*b*-PILi living ends were finally deactivated by addition of degassed methanol.

Analysis and Characterization Techniques. *Static and Dynamic Light Scattering Measurements*. They were performed in tetrahydrofuran (THF) using the ALV (Langen-FRG) apparatus consisting of an automatic goniometer table, a digital rate meter, and a temperature control of the sample cell within $t \pm 0.1$ °C. The scattered light of a vertically polarized $\lambda_0 = 4880$ Å argon laser (Spectra-Physics 2020, 3 W, operating around 0.3 W) was measured at different angles in the range of 40°−150° corresponding to $1.2 \times 10^{-3} < q/\text{Å} < 3.3 \times 10^{-3}$ where $q = (4\pi n/\lambda_0)\sin(\theta/2)$, θ is the scattering angle, and n is the refractive index of the medium (n = 1.41, for THF). The reduced elastic scattering $I(q)/KC$, with $K = 4\pi^2 n_0 (dn/dc)^2 (I_0^{90°}/R^{90°})/\lambda_0^4 N_A$, was measured in steps of 2° in the scattering angle, where n_0 is the refractive index of the standard (toluene); $I_0^{90°}$ and $R^{90°}$ are the intensity and the Rayleigh ratio of the standard at $\theta = 90°$, respectively; dn/dc is the increment of the refractive index; C is the concentration, expressed in g/cm^3; and $I(q)$ is the intensity scattered by the sample. All elastic intensities were calculated according to standard procedures using THF as the standard with known absolute scattering intensity.

For the dynamic properties, the experiments were carried out in steps of 20° in the scattering angle. The ALV5000 autocorrelator (ALV, FRG) was used to compute the autocorrelation functions $I(q,t)$ from the scattered intensity data. The autocorrelation functions of the scattered intensity, deduced from the Siegert relation,[44] were analyzed by means of the cumulant method and Contin analysis to give the effective diffusion coefficient $D = \Gamma(q)/q^2$ as a function of the scattering angle or the square of wave vector q^2 and ultimately the hydrodynamic radius $R_H = k_B T/(6\pi\eta D)$, where η is the viscosity of the medium.

Atomic Force Microscopy (AFM). Samples for AFM analysis were prepared by solvent-casting at ambient temperature conditions by spin-coating on substrates starting from solutions in dichloromethane. Practically, 20 μL of a dilute solution (0.01 wt %) was spin-cast on a 1 × 1 cm^2 on a highly oriented pyrolytic graphite (HOPG). Samples were analyzed after complete evaporation of the solvent at room temperature. All AFM images were recorded in air with a Dimension microscope (Digital Instruments, Santa Barbara, CA), operated in tapping mode. The probes were commercially available silicon tips with a spring constant of 40 N/m, a resonance frequency lying in the 270−320 kHz range, and a radius of curvature in the 10−15 nm range. In this work, both the topography and the phase signal images were recorded with the highest sampling resolution available, i.e., 512 × 512 data points.

Small-Angle X-ray Scattering. Small-angle X-ray scattering (SAXS) was used to identify the types of structures and domain spacing in nano-organized films made from comblike copolymers. The experiments were performed using Cu K radiation (1.54 Å wavelength) using a Nanostar from Bruker AXS (operating at 40 kV, 35 mA). A CCD detector (Siemens Hi-Star), at a sample/detector distance of 106.2 cm, was used to record scattering patterns.

Other Characterization Techniques and Measurements. ^{1}H NMR spectra were recorded in $CDCl_3$ on a BrukerAvance 400 MHz FT apparatus. Size exclusion chromatography (SEC) analysis in THF (distilled from CaH_2) was performed at 25 °C at a flow rate of 0.7 mL/min using a Varian apparatus equipped with refractive index/laser light scattering (He/Ne, λ = 632.8 nm, 5 mW) dual detection (Wyatt Technology) and fitted with four TSK columns (300 × 7.7 mm^2, 250, 1500, 10^4, 10^5 Å). dn/dc of the comb copolymers in THF were determined from dn/dc values of PI and PS, respectively 0.120 and 0.181 at 632.8 nm, taking into account their weight fractions. This yields dn/dc of 0.165 and 0.135 for PCEVE-*g*-(PS,PI) (**2a**, **2b**).

Results and Discussion

Synthesis of PCEVE-*g*-(PS,PI). The synthetic procedure used for the preparation of comblike copolymers with randomly distributed branches of polystyrene and polyisoprene is illustrated in Scheme 1. In a first step a poly(chloroethyl vinyl ether)-*g*-polystyrene, PCEVE-*g*-PS*, with only partial substitution of the chloride groups of CEVE units was first prepared according to a procedure previously reported.[8,24,43] In this study, polystyryllithium, PSLi, with $\overline{M}_n$ = 8960 g/mol ($\overline{DP}_{n(PS)}$ = 86) and $\overline{M}_w/\overline{M}_n$ = 1.02 was prepared and added incrementally onto a PCEVE of $\overline{DP}_n$ = 230, dissolved in tetrahydrofuran. Sampling of the solution with time allowed monitoring by size exclusion chromatography (SEC) the grafting yield, using both refractive index (RI) and light scattering (LS) detections. PSLi addition was stopped when reaching a PS grafting rate of about 50%, which means that half of the chloride atoms of the PCEVE have been substituted by a PS chain. After purification by selective precipitation in cyclohexane/heptane mixture (1:5), the PCEVE-*g*-PS* comb was further characterized by proton NMR, size exclusion chromatography (SEC), and light scattering (LS). The characteristics of the corresponding PCEVE-*g*-PS* (**1**) are given in Table 1.

The synthesis of comblike copolymers with randomly distributed PS and PI branches was achieved in a second step by a "grafting onto" reaction involving the addition of living polyisoprene (PI) chains end-capped by diphenylethylene (PIDLi, with D for diphenylehylene) onto the PCEVE-*g*-PS* (**1**) in toluene solution. To achieve complete PI grafting, i.e., one PI graft per remaining CEVE unit, PIDLi was added in excess with respect to CEVE residual units. The ungrafted polyisoprene was then removed from the PCEVE-*g*-(PS,PI) comblike copolymer by selective precipitation into a dicloromethane/methanol mixture (1:4). The SEC profiles of PCEVE-*g*-PS* (**1**) and PCEVE-*g*-(PS,PI) (**2**) samples show narrow monomodal

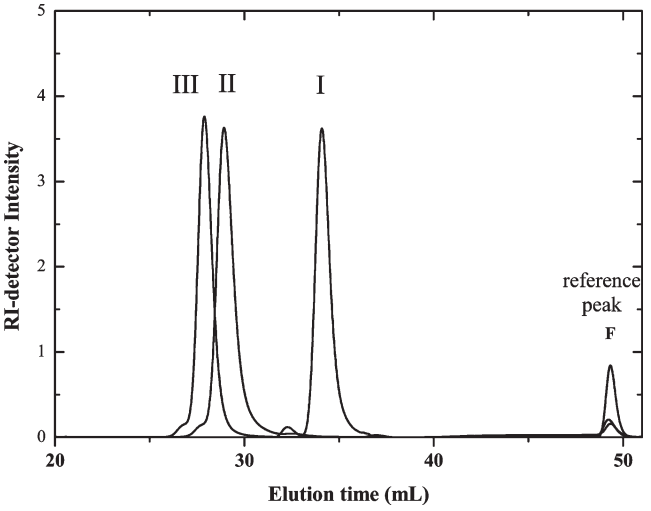

Figure 2. SEC traces recorded at the different building stages of the synthesis of comb copolymers: (I) $PCEVE_{230}$, (II) $PCEVE_{230}$-*g*-PS_{86} (**1**), (III) $PCEVE_{230}$-*g*-(PS_{86}, PI_{98}) (**2b**). Peak F is the reference peak for calculation.

distributions, with M_w/M_n values being less than 1.10 (see Figure 2). The characteristics of the different PCEVE-*g*-(PS,PI) combs are collected in Table 1. The chemical composition into styrene and isoprene of the comb copolymers, determined by ^{1}H NMR, corresponds to polystyrene and polyisoprene grafting ratio of 45% and 55% with respect to the total number of grafts. Theoretical molar masses of the PS,PI combs, calculated from the $\overline{DP}_n$s of the PCEVE backbone and of the PS and PI grafts, assuming one graft per CEVE unit, are indicated in Table 1. They can be compared to experimental values measured by static light scattering (SLS) using a $dn/dc = 0.181$ for PCEVE-*g*-PS* (**1**) and $dn/dc = 0.165$ and 0.135 for PCEVE-*g*-PS,PI (**2a**) and (**2b**), respectively. The good agreement observed suggests an almost quantitative substitution of the whole CEVE units.

AFM Imaging of Comb Copolymers. Dilute solutions of the synthesized comb (co)polymers were prepared in methylene dichloride (0.1 g/L), a good solvent for both the PS and PI grafts, and spin-cast on graphite in order to observe individual macromolecules. Figure 3 shows the AFM images of combs $PCEVE_{230}$-*g*-(PS_{86},PI_{98}) (**2b**). They reveal individual macromolecules lying flat on the substrate and which appear as uniform object with an ovoïdal conformation. Their homogeneity in size confirms the narrow size distribution observed by SEC. A statistical analysis of the AFM image of sample **2b** shows that the average contour length L and the width l of the PS,Pi comb are $L = 51$ nm and $l = 22$ nm whereas their height is only of 1.5 nm, indicating that they are completely flattened on the substrate due to the good affinity of PI and PS grafts with graphite. In contrast to previous AFM studies performed on PCEVE-*g*-(PS-*b*-PI) comb copolymers,[31] a phase segregation within the macromolecules is not observed, suggesting that PS and PI are still in admixture in a common phase due to their random distribution along the comb backbone.

Solution Properties. The solution properties of PCEVE-*g*-PS* (**1**) and PCEVE-*g*-(PS,PI) combs (**2a**, **2b**) were investigated using static and dynamic light scattering in THF, a common good solvent for the PCEVE backbone, the polystyrene, and the polyisoprene branches.

Figure 4 shows the typical normalized autocorrelation functions for the PCEVE-*g*-PS* (**1**) and PCEVE-*g*-(PS, PI) (**2a**) at $t = 25$ °C. The CONTIN analysis of the autocorrelation functions shows a monomodal decay time distribution

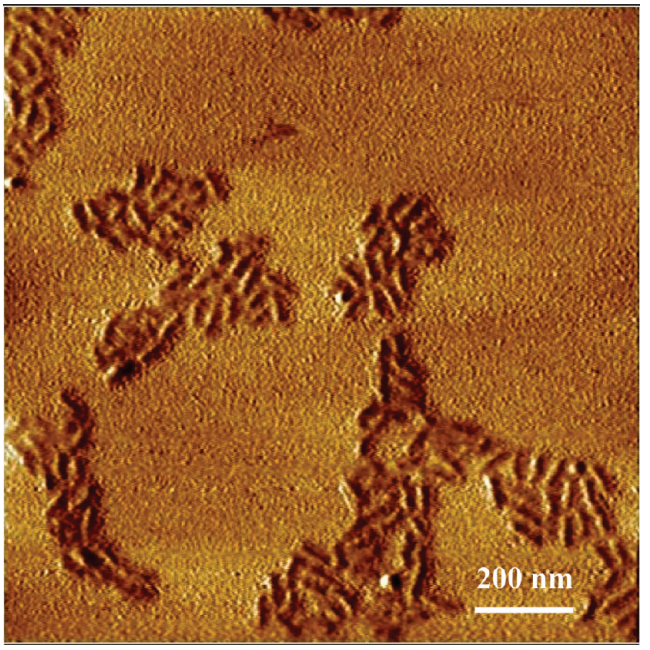

Figure 3. AFM tapping phase image of $PCEVE_{230}$-*g*-(PS_{86},PI_{98}) (**2b**) obtained from deposit on graphite of their methylene dichloride solution.

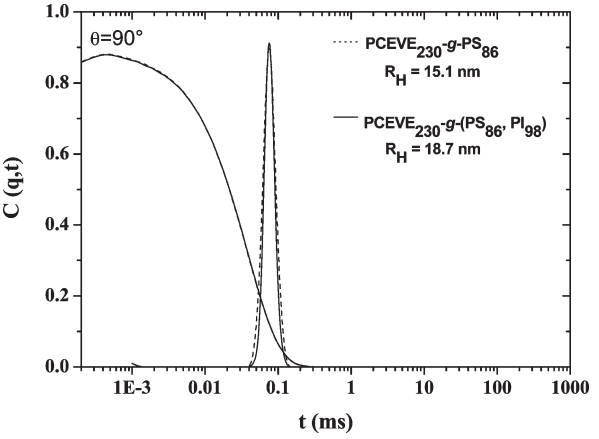

Figure 4. Normalized field correlation and corresponding relaxation times at $\theta = 90°$ for a concentration of 3.3 g/L solution in THF, at the temperature of 25 °C for (a) $PCEVE_{230}$-*g*-PS_{86} (**2a**) and (b) $PCEVE_{230}$-*g*-(PS_{86}, PI_{98}) (**2b**).

Table 2. Characteristics and Dimensions of the Poly(chloroethyl vinyl ether-*g*-polystyrene* (1) and Poly(chloroethyl vinyl ether-*g*-(polystyrene, polyisoprene) (2a, 2b) in Tetrahydrofuran at 25 °C

ref no.	constitutive blocks, $\overline{DP}_n$ PCEVE−(PS,PI)	R_{H0} (nm)[a]	R_g (nm)[b]	R_g/R_{H0}
1	230−(86, 0)	15.1	25.0	1.65
2a	230−(86, 57)	16.6	23.7	1.43
2b	230−(86, 98)	18.7	23.5	1.26

[a] R_{H0} determined using DLS extrapolated to infinite dilution ($C \rightarrow 0$). [b] R_g determined using SLS from the Zimm method.

at all scattering angles. Typical result is illustrated in Figure 4 and shows for the two samples a very narrow size distribution. This result confirms the presence in solution of single comblike objects corresponding to isolated macromolecules with very low dispersity as observed by SEC and AFM. The corresponding apparent hydrodynamic radii calculated according to Stokes−Einstein relation range from 16.6 (**1**) to 18.7 nm (**2**). The hydrodynamic radii of other comb samples are collected in Table 2. The very small hydrodynamic radii

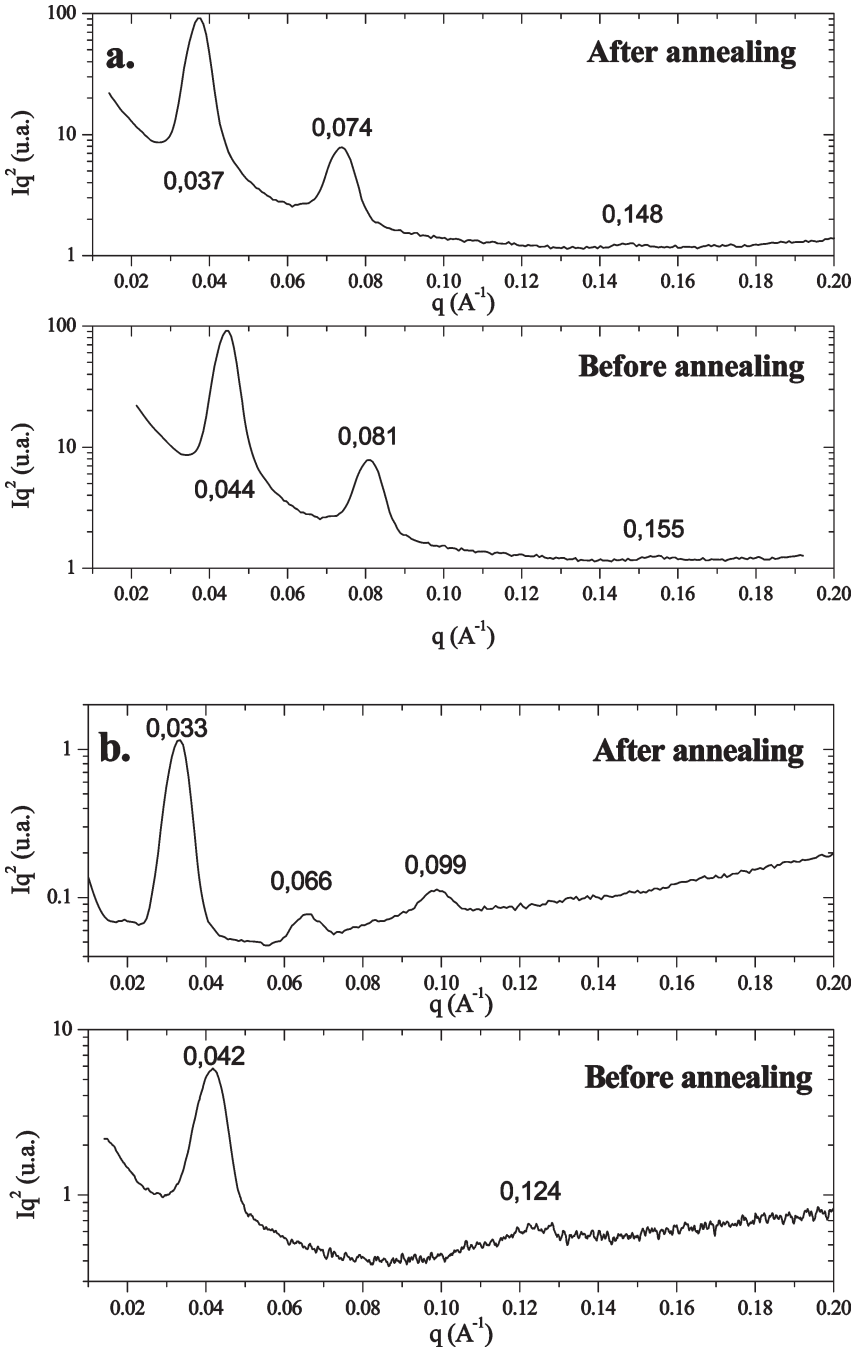

Figure 5. SAXS intensity $Iq^2(q)$ as a function of q for (a) PCEVE$_{230}$-*g*-(PS$_{86}$, PI$_{57}$) (**2a**) and (b) PCEVE$_{230}$-*g*-(PS$_{86}$, PI$_{98}$) (**2b**) comb copolymers.

value confirms the highly compact structure of these high molar mass macromolecules.

The radius of gyration of the comb macromolecules measured using static light scattering (SLS) in THF is given in Table 2 . The Berry plots obtained for the PCEVE$_{230}$-*g*-PS$_{86}$* (**1**) and PCEVE$_{230}$-*g*-(PS$_{86}$, PI$_{98}$) (**2b**) combs are given in Figure S1 as Supporting Information. The R_g/R_{H0} ratio, given in Table 2, is higher for the PCEVE-*g*-PS* (**1**) than for the PCEVE-*g*-(PS,PI) comb copolymers (**2a** and **2b**), and it decreases in the copolymer series when decreasing the length of the PI branches. This can be explained either by the formation of more compact objects with increasing graft density along the backbone for the fully grafted PS,PI comb copolymers or by a lower length/diameter ratio, implying that the molecules become more oblong and less rod-shaped.

Bulk Properties. SAXS experiments were performed on PCEVE-*g*-(PS,PI) comb copolymers films at two distinct volume fraction compositions to examine a possible microphase separation between PS and PI branches and to determine the corresponding nano-organized phase. In addition, a similar SAXS study was performed (i) on PCEVE-*g*-(PS-*b*-PI) combs with diblock PS-*b*-PI branches (**3a**, **3b**, **3c**), previously prepared for investigating their solution behavior,[31] and (ii) on synthesized linear diblock PS-*b*-PI copolymers. The molar mass and composition of the latter was close to one PS-*b*-PI branch of combs (series **3**) and to one PS + one PI branches of combs of (series **2**). The sample films were prepared on glass plates by solvent evaporation of their THF solution deposits. SAXS measurements were performed before and after samples annealing at 120 °C for 48 h.

Comblike Copolymers with Randomly Distributed PS and PI Branches. Figure 5a,b illustrates the typical scattered intensity $Iq^2(q)$ as a function of scattering vector q ($= 4\pi/\lambda \sin(\theta/2)$, with θ being the scattering angle), for the

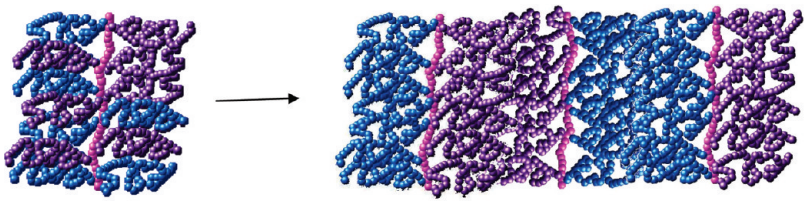

Figure 6. Schematic representation of inter- and intramolecular self-organization of comb copolymer macromolecules with randomly distributed PS and PI branches in thin films.

Table 3. Characteristics of Comblike Copolymers and Linear Diblock Copolymers Thin Films Determined by Small-Angle X-ray Scattering

ref no.	$\overline{DP}_n$	$\Phi_{vPS/PI}$	χN_T[a]	d-spacing (nm)[b]	$D_{lam,th}$ (nm)[c]	morphology
			PCEVE-*g*-(PS,PI)			
2a	230−(86, 57)	60/40	15.9	14.3/17.0	21.6	lamellar
2b	230−(86, 98)	48/52	20.2	15.0/19.0	24.0	lamellar
			PCEVE-*g*-(PS-*b*-PI)			
3a	230−(106−21)	87/13	14.2		20.4	disordered
3b	230-(122−78)	67/33	22.3	16.1/17.4	26.0	lamellar
3c	230−122−192	45/55	34.5	17.9/27.3	31.2	lamellar
			PS-*b*-PI (linear)			
L1	115−65	70/30	20.1	19.0/19.0[d]		hexagonal
L2	115−175	46/54	32.3	22.4/22.4	30.0	Lamellar

[a] χN_T determined using the relation $\chi N_T = -0.0522 + 48.8/T$ (K). [b] d-spacing determined using the Bragg relation $d_{lam} = 2\pi/q$ for a lamellar morphology obtained from the SAXS experiments (before annealing/after annealing). [c] $d_{lam,th}$ = theoric lamellar distance = $4x(R_{g,PS} + R_{g,PI})$. We assume that each block (PS and PI) has a Gaussian conformation.[45] [d] d-spacing determined from the hexagonal phase $d_{hex} = 4\pi/(q\sqrt{3})$.

$PCEVE_{230}$-*g*-(PS_{86},PI_{57}) (**2a**) and $PCEVE_{230}$-*g*-(PS_{86},PI_{98}) (**2b**) combs. The overall scattering intensity and peak resolution are significantly improved by annealing, favoring a better branches organization and an increase of the *d*-spacing. Peak positions are consistent with a lamellar microstructure for both samples. This result confirms that despite the random distribution of PS and PI branches attached along the PCEVE backbone, segregation between polystyrene and polyisoprene takes place and results in microphase separation similarly to symmetric linear PS−PI block copolymer system. This means that the PS and PI branches are able to rotate around the backbone to self-assemble in microdomains as illustrated in Figure 6.

The theoretical radii of gyration corresponding respectively to PS and PI branches in PCEVE-*g*-(PS-*b*-PI) combs was estimated using the scaling laws given below for PS and PI blocks in good solvent conditions:[45]

$$R_g = 2.45 \times 10^{-2} M_{PS}^{0.546} \text{ nm} \quad (1)$$

$$R_g = 2.75 \times 10^{-2} M_{PI}^{0.513} \text{ nm} \quad (2)$$

In this model, it is assumed that PS and PI branches adopt a Gaussian conformation and are independent from each other at the junction point. This yields $d_{lam,th}$ = 21.6 nm for $PCEVE_{230}$-*g*-(PS_{86}, PI_{57}) (**2a**) and $d_{lam,th}$ = 24.0 nm for $PCEVE_{230}$-*g*-(PS_{86},PI_{98}) (**2b**). These values are notably higher than experimentally observed for *d*-spacing, i.e., 10.2 and 9.1 nm for **2a** and **2b**, respectively (see Table 3). This result can be explained by the fact that the dimensions in the melt are always smaller than in good solvent. It supports also that branches adopt a Gaussian conformation with interdigitation between polyisoprene branches and between polystyrene branches belonging to adjacent comb copolymers. The dimension characteristics and morphology parameters of the comblike block copolymers are collected Table 3.

Comblike Block Copolymers and Linear Block Copolymers. The typical scattered intensity $Iq^2(q)$ as a function of scattering vector q of comb block copolymers PCEVE-*g*-(PS-*b*-PI)[31] are shown in Figure 7 for three comb copolymers with the same backbone length and PS-*b*-PI diblock branches with identical polystyrene block and different polyisoprene block length: $PCEVE_{230}$-*g*-(PS_{122}-*b*-PI_{192}) (**3c**), $PCEVE_{230}$-*g*-(PS_{106}-*b*-PI_{78}) (**3b**), and $PCEVE_{230}$-*g*-(PS_{106}-*b*-PI_{21}) (**3a**). This corresponds to a polystyrene volume fraction of 45%, 67%, and 87%, respectively. For the comblike block copolymers with the longer polyisoprene block, $PCEVE_{230}$-*g*-(PS_{122}-*b*-PI_{192}) (**3c**), the maxima of the peak positions are consistent with a lamellar organization. Annealing results in a better signal resolution or a better statistics with the appearance of a new peak, whereas q_{max} shifts to a smaller value and corresponds to an increase of *d*-spacing from 19.3 to 27.3 nm (Table 3). For the $PCEVE_{230}$-*g*-(PS_{106}-*b*-PI_{78}) (**3b**) the Bragg peaks (maxima) position before annealing also suggests lamellar-type morphology. However, in this case the morphology could not be improved by annealing, which resulted in PI block cross-linking. No Bragg peak is observed for the comb copolymers with the shorter PI block, $PCEVE_{230}$-*g*-(PS_{106}-*b*-PI_{21}) (**3a**). This can be attributed to a too weak phase separation tendency (χN_T for a PS_{106}-*b*-PI_{21} branch = 14.2) that does not allow block segregation and oriented macromolecules self-organization.

Radii of gyration calculated for combs **3a** and **3b** from relations 1 and 2, assuming that each block (PS and PI) has a Gaussian conformation and evolves independently from each other at the junction point are indicated in Table 3. The obtained $d_{lam,th}$ values, 26.0 and 31.2 nm respectively for $PCEVE_{230}$-*g*-(PS_{122}-*b*-PI_{192}) (**3c**) and $PCEVE_{230}$-*g*-(PS_{106}-*b*-PI_{78}) (**3b**), are again much larger than the *d*-spacing experimentally determined; **3a** = 11.7 nm and **3b** = 12.3 nm.

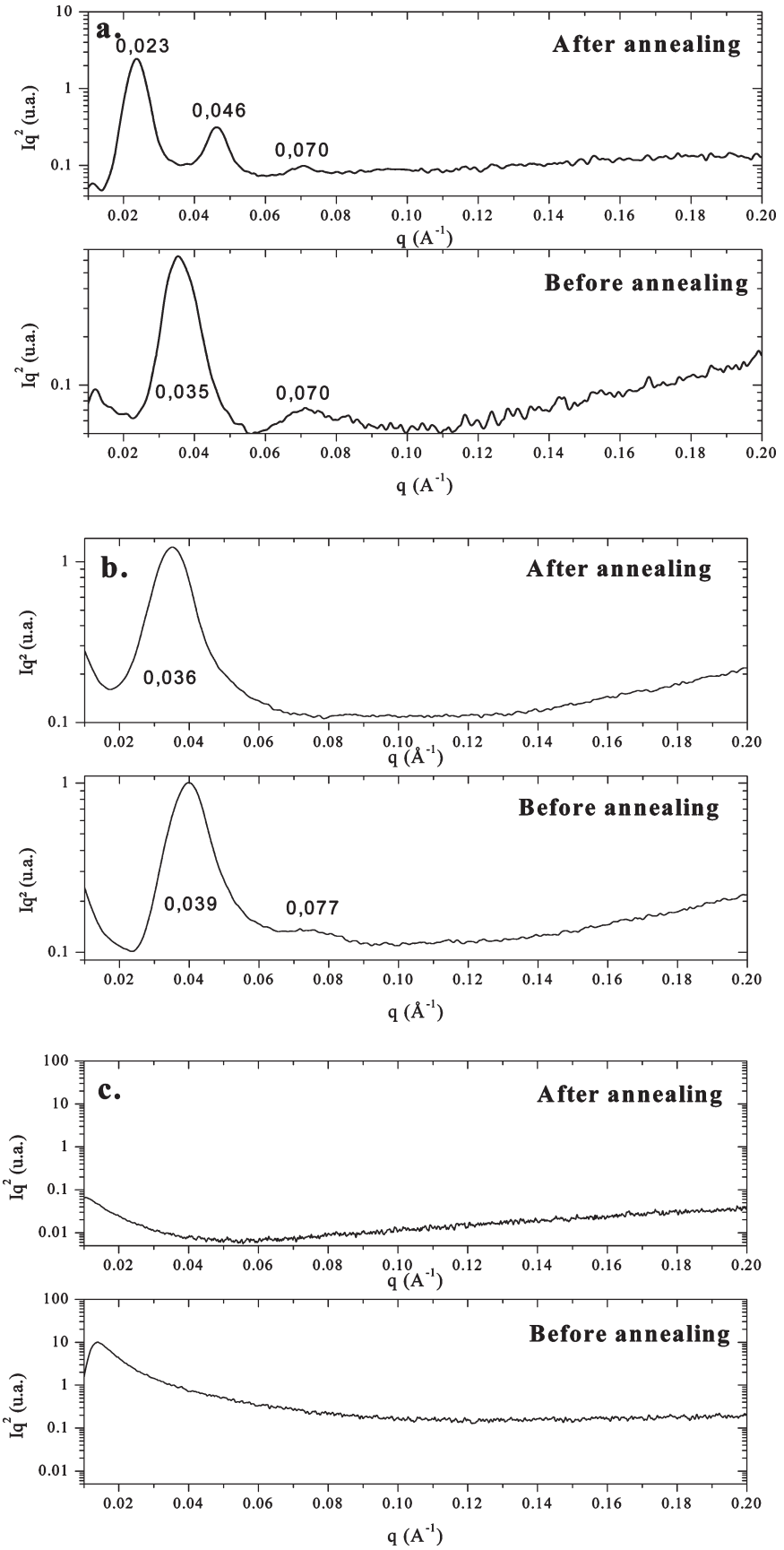

Figure 7. SAXS intensity $Iq^2(q)$ as a function of q for (a) $PCEVE_{230}$-*g*-(PS_{122}-*b*-PI_{192}) (**3a**), (b) $PCEVE_{230}$-*g*-(PS_{106}-*b*-PI_{78}) (**3b**), and (c) $PCEVE_{230}$-*g*-(PS_{106}-*b*-PI_{21}) (**3c**) comb copolymers.

This indicates that again branches adopt a Gaussian conformation with an interdigitation between the external PI blocks of neighboring PCEVE-*g*-(PS-*b*-PI) comb copolymers. The dimensions and structural characteristics of the comb copolymers with PS-*b*-PI diblock branches are collected in Table 3.

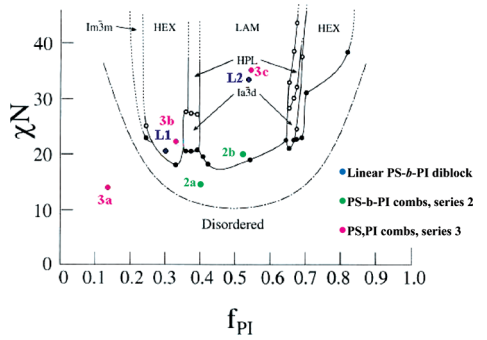

Figure 8. Experimental phase diagram for linear diblock copolymers PS-*b*-PI according Bates. Reprinted with permission from ref 46. Theoretical positions for comblike block copolymers (a) $PCEVE_{230}$-*g*-(PS_{122}-*b*-PI_{192}) (**3c**), (b) $PCEVE_{230}$-*g*-(PS_{122}-*b*-PI_{78}) (**3b**), (c) $PCEVE_{230}$-*g*-(PS_{106}-*b*-PI_{21}) (**3a**), and linear diblock copolymers (a′) PS_{115}-*b*-PI_{175} (**L2**) and (b′) PS_{115}-*b*-PI_{65} (**L1**).

In Figure 8 we have reported on the phase diagram established for linear PS-*b*-PI diblock copolymers by Bates,[46] the comb copolymer systems PCEVE-*g*-(PS,PI) (**2a**, **2b**), and PCEVE-*g*-(PS-*b*-PI) (**3a**, **3b**, **3c**) on the basis of their volume fraction composition and χN_T values. The latter were calculated considering the equivalent diblock copolymer systems corresponding to one PS branch + one PI branch for series 2 and to one PS-*b*-PI branch for series 3. Systems **2a** and **2b** which exhibit a lamellar morphology are located within or close to the lamellar domain of linear diblocks. This is also the case for system **3c** which is within the linear diblock lamellar domain, whereas as predicted by the phase diagram, system **3a** lays in the disordered domain. In contrast, the $PCEVE_{230}$-*g*-(PS_{122}-*b*-PI_{78}) (**3b**), which also shows a lamellar morphology (Figure 7), lays in the hexagonal morphology domain predicted for the corresponding linear diblock copolymers, as is confirmed by the hexagonal structure observed for PS_{115}-*b*-PI_{65} (**L1**) (see Figure S2 in Supporting Information).

Conclusion

The synthesis of PCEVE-*g*-(PS,PI) comblike block copolymers of different chemical composition with randomly distributed PS and PI branches was successfully achieved by a grafting onto approach. Light scattering experiments and AFM were used to highlight the characteristics of these macromolecules as isolated object in solution and in the solid. AFM experiments show that isolated PCEVE-*g*-(PS,PI) combs adsorbed on graphite are uniform objects with an ovoïdal conformation. In contrast to previously observed for the case of PCEVE-*g*-(PS-*b*-PI) copolymers with PS-*b*-PI diblock branches, PCEVE-*g*-(PS,PI) are organized in a single phase constituted by the randomly distributed PS and PI branches. However, in thin films, the comb macromolecules reorganize intra- and intermolecularly to yield biphasic structures constituted by the segregation of PS and PI branches. This is very similar to the behavior of PCEVE-*g*-(PS-*b*-PI) copolymers with PS-*b*-PI diblock branches that form lamellar-type biphasic morphology for all composition examined. Further studies are in progress to investigate the morphology of PCEVE-*g*-(PS,PI) comb copolymers with more asymmetric PS and PI composition or volume fraction and compare it with the morphology reported for linear PS-*b*-PI copolymers of the same composition.

Supporting Information Available: Berry plots for $PCEVE_{230}$-*g*-PS_{86} and $PCEVE_{230}$-*g*-(PS_{86}, PI_{98}) in THF at 25 °C and SAXS intensity $Iq^2(q)$ as a function of q for PS_{115}-*b*-PI_{175} and PS_{115}-*b*-PI_{65} linear diblock copolymers. This material is available free of charge via the Internet at http://pubs.acs.org.

References and Notes

(1) Park, M.; Harrison, C.; Chaikin, P. M.; Register, R. A.; Adamson, D. H. *Science* **1997**, *276*, 1401–1404.
(2) Stupp, S. I.; Braun, P. V. *Science* **1997**, *277*, 1242.
(3) Koutalas, G.; Iatrou, H.; Lohse, D. J.; Hadjichristidis, N. *Macromolecules* **2005**, *38*, 4996–5001.
(4) Hirao, A.; Hayashi, M.; Loykulnant, S.; Sugiyama, K.; Ryu, S. W.; Haraguchi, N.; Matsuo, A.; Higashihara, T. *Prog. Polym. Sci.* **2005**, *30*, 111–182.
(5) Ishizu, K. *Polym. J. (Tokyo, Jpn.)* **2004**, *36*, 775–792.
(6) Beers, K. L.; Gaynor, S. G.; Matyjaszewski, K.; Sheiko, S. S.; Moeller, M. *Macromolecules* **1998**, *31*, 9413–9415.
(7) Lubnin, A. V.; Kennedy, J. P. *J. Macromol. Sci., Pure Appl. Chem.* **1994**, *A31*, 1943–1953.
(8) Schappacher, M.; Deffieux, A. *Macromol. Chem. Phys.* **1997**, *198*, 3953–3961.
(9) Weisberg, D. M.; Gordon, B.III; Rosenberg, G.; Snyder, A. J.; Benesi, A.; Runt, J. *Macromolecules* **2000**, *33*, 4380–4389.
(10) Zhang, M.; Breiner, T.; Mori, H.; Muller, A. H. E. *Polymer* **2003**, *44*, 1449–1458.
(11) Li, Y. G.; Shi, P. J.; Zhou, Y.; Pan, C. Y. *Polym. Int.* **2004**, *53*, 349–354.
(12) Cheng, Z.; Zhu, X.; Fu, G. D.; Kang, E. T.; Neoh, K. G. *Macromolecules* **2005**, *38*, 7187–7192.
(13) Christodoulou, S.; Iatrou, H.; Lohse, D. J.; Hadjichristidis, N. *J. Polym. Sci., Part A: Polym. Chem.* **2005**, *43*, 4030–4039.
(14) Koutalas, G.; Lohse, D. J.; Hadjichristidis, N. *J. Polym. Sci., Part A: Polym. Chem.* **2005**, *43*, 4040–4049.
(15) Wang, W. P.; You, Y. Z.; Hong, C. Y.; Xu, J.; Pan, C. Y. *Polymer* **2005**, *46*, 9489–9494.
(16) Zhang, M.; Muller, A. H. E. *J. Polym. Sci., Part A: Polym. Chem.* **2005**, *43*, 3461–3481.
(17) Han, D. H.; Pan, C. Y. *Macromol. Chem. Phys.* **2006**, *207*, 836–843.
(18) Li, X.; Ji, J.; Shen, J. *Polymer* **2006**, *47*, 1987–1994.
(19) Ostmark, E.; Harrison, S.; Wooley, K. L.; Malmström, E. E. *Biomacromolecules* **2007**, *8*, 1138–1148.
(20) Lessard, B.; Maricia, M. *Macromolecules* **2008**, *41*, 7870–7880.
(21) Quemener, D.; Le Hellaye, M.; Bissett, C.; Davis, T. P.; Barner-Kowollik, C.; Stenzel, M. H. *J. Polym. Sci., Part A: Polym. Chem.* **2008**, *46*, 155–173.
(22) Wan, L. S.; Lei, H.; Ding, Y.; Fu, L.; Li, J.; Xu, Z. K. *J. Polym. Sci., Part A: Polym. Chem.* **2009**, *47*, 92–102.
(23) Pitsikalis, M.; Woodward, J.; Mays, J. W.; Hadjichristidis, N. *Macromolecules* **1997**, *30*, 5384–5389.
(24) Schappacher, M.; Billaud, C.; Paulo, C.; Deffieux, A. *Macromol. Chem. Phys.* **1999**, *200*, 2377–2386.
(25) Ishizu, K.; Satoh, J.; Toyoda, K.; Sogabe, A. *J. Mater. Sci.* **2004**, *39*, 4295–4300.
(26) Neiser, M. W.; Muth, S.; Kolb, U.; Harris, J. R.; Okuda, J.; Schmidt, M. *Angew. Chem., Int. Ed.* **2004**, *43*, 3192–3195.
(27) Nguyen, S.; Marchessault, R. H. *Macromol. Biosci.* **2004**, *4*, 262–268.
(28) Tang, D.; Lin, J.; Lin, S.; Zhang, S.; Chen, T.; Tian, X. *Macromol. Rapid Commun.* **2004**, *25*, 1241–1246.
(29) Ten Brinke, G.; Ikkala, O. *Chem. Rec.* **2004**, *4*, 219–230.
(30) Harris, H. V.; Holder, S. J. *Polymer* **2006**, *47*, 5701–5706.
(31) Lanson, D.; Schappacher, M.; Deffieux, A.; Borsali, R. *Macromolecules* **2006**, *39*, 7107–7114.
(32) Lanson, D.; Schappacher, M.; Borsali, R.; Deffieux, A. *Macromolecules* **2007**, *40*, 5559–5564.
(33) Zhou, J.; Wang, L.; Yang, Q.; Dong, X.; Yu, H. *Colloid Polym. Sci.* **2007**, *285*, 1369–1376.
(34) Kim, K. H.; Lee, J. C.; Lee, J. *Macromol. Biosci.* **2008**, *8*, 339–346.
(35) Runge, M. B.; Dutta, S.; Bowden, N. B. *Macromolecules* **2006**, *39*, 498–508.
(36) Lanson, D.; Ariura, F.; Schappacher, M.; Borsali, R.; Deffieux, A. *Macromol. Res.* **2007**, *15*, 173–177.
(37) Lanson, D.; Schappacher, M.; Borsali, R.; Deffieux, A. *Macromolecules* **2007**, *40*, 9503–9509.
(38) Palyulin, V. V.; Potemkin, I. I. *J. Polym. Sci., Ser. A* **2007**, *49*, 473–481.
(39) Runge, M. B.; Bowden, N. B. *J. Am. Chem. Soc.* **2007**, *129*, 10551–10560.
(40) Liu, Y. T.; Li, Z. W.; Lu, Z. Y.; Li, Z. S. *Gaodeng Xuexiao Huaxue Xuebao* **2008**, *29*, 1200–1204.
(41) Qi, H.; Zhong, C. *J. Phys. Chem. B* **2008**, *112*, 10841–10847.

(42) Yi, Z.; Liu, X.; Jiao, Q.; Chen, E.; Chen, Y.; Xi, F. *J. Polym. Sci., Part A: Polym. Chem.* **2008**, *46*, 4205–4217.
(43) Schappacher, M.; Deffieux, A. *Makromol. Chem., Rapid Commun.* **1991**, *12*, 447–53.
(44) Siegert, A. *J. MIT Rad. Lab. Rep.* **1943**, 465.
(45) Fetters, L. J.; Hadjichristidis, N.; Lindner, J. S.; Mays, J. W. *J. Phys. Chem. Ref. Data* **1994**, *23*, 619–40.
(46) Khandpur, A. K.; Foerster, S.; Bates, F. S.; Hamley, I. W.; Ryan, A. J.; Bras, W.; Almdal, K.; Mortensen, K. *Macromolecules* **1995**, *28*, 8796–806.